Strain effects on the electronic structure of SrTiO_{3}: Toward high electron mobilities

A. Janotti, D. Steiauf, and C. G. Van de Walle

Phys. Rev. B **84**, 201304 — Published 8 November 2011

DOI: 10.1103/PhysRevB.84.201304

Strain effects on the electronic structure of $SrTiO_3$: Towards high electron mobilities

A. Janotti, D. Steiauf, and C. G. Van de Walle
Materials Department, University of California, Santa Barbara, CA 93106-5050
(Dated: October 19, 2011)

Using the screened hybrid functional of Heyd, Scuseria, and Ernzerhof (HSE) we explore the effects of strain on the energetic ordering and effective mass of the lowest conduction-band states in $SrTiO_3$. We predict that biaxial stress in the (001) or (110) planes result in the lowest-energy conduction-band state having significantly smaller electron mass in the in-plane directions compared to the unstrained $SrTiO_3$, thus suggesting that pseudomorphic growth is a promising route to increasing the electron mobility in epitaxial films. We propose possible substrates that may lead to $SrTiO_3$ films with enhanced electron mobilities, and report deformation potentials that allow accurate prediction of conduction-band splittings for arbitrary strain configurations.

PACS numbers: 71.20.Ps,71.70.Fk,73.50.Dn

$SrTiO_3$ has attracted great attention ever since charge modulation and the formation of a two-dimensional electron gas (2DEG) at the $SrTiO_3/LaAlO_3$ interface have been reported.[1–3] $SrTiO_3$ has a wide band gap and can easily be doped n-type. Epitaxial $SrTiO_3$ films with high structural quality have been shown to exhibit low-temperature electron mobilities exceeding 30,000 $cm^2V^{-1}s^{-1}$.[4] Despite this impressive recent progress, many features of the band structure remain unknown. For example, reported experimental[5,6] and theoretical[7–10] values for the electron effective mass range from $1.0m_0$ to $16m_0$.

Given the growing interest in electronic transport in epitaxial heterostructures that combine $SrTiO_3$ with other multifunctional oxides, it is important to know how strain affects the electronic properties or, more specifically, the electron mobility in $SrTiO_3$. Recent experiments[11] have shown that application of external compressive uniaxial stress to La-doped $SrTiO_3$ films results in significant enhancements of the electron mobility. In general, pseudomorphic growth offers great opportunities for strain engineering: epitaxial films have their in-plane lattice constant determined by the substrate as long as the number of atomic layers remains below a critical layer thickness. The resulting strain in the epitaxial layer can greatly affect the absolute energy, degeneracy, and ordering of the band-edge states. In this work we show that strain allows tuning the ordering of the lowest conduction-band states in $SrTiO_3$ epitaxial films, and thereby modifying the electron effective mass and mobility. In particular, $SrTiO_3$ layers under biaxial tensile stress in the (001) plane, or biaxial stress in the (110) plane, either tensile or compressive, are predicted to exhibit small effective mass in the directions that are relevant for the electron transport.

The calculations are based on generalized Kohn-Sham theory[12] using the screened hybrid functional of Heyd, Scuseria, and Ernzerhof (HSE)[13] as implemented in the VASP code.[14,15] We use the Hartree-Fock mixing parameter of 25% and screening parameter ω=0.2 $Å^{-1}$. The electron-ion interactions are treated in the projector augmented wave (PAW) approach,[16,17] and the wave functions are expanded in plane waves with cutoff up to 600 eV. Integrations over the Brillouin zone are replaced by sums over special k points, with a grid of 4×4×4 for the primitive cell (containing 5 atoms) of cubic $SrTiO_3$. We focus on cubic $SrTiO_3$, since it is the stable phase at room temperature and the transition to the lower-symmetry tetragonal phase occurs below 105 K.[18,19] The effects of biaxial stress in the (001) and (110) planes are investigated by constraining the in-plane lattice parameter (leading to an in-plane strain $\varepsilon_\parallel$) and allowing the lattice to relax along the perpendicular direction, resulting in a strain $\varepsilon_\perp$. The presence of biaxial strain can cause lower-symmetry phases, which would involve rotations of the TiO_6 octahedra, to become stable at higher temperatures.[20,21] While a full study of these effects is beyond the scope of the present work, we have performed test calculations for $SrTiO_3$ biaxially strained in the (001) plane in which TiO_6 rotations around the [001] axis were allowed. We find that TiO_6 rotations change the calculated splitting of the lowest energy conduction-band states by less than 4 meV and effective masses by less than 5%.

The calculated lattice constant for the cubic $SrTiO_3$ is 3.905 Å, in good agreement with recent calculations[22] and with the experimental value of 3.900 Å.[18,19] In Fig. 1 we show the calculated band structure of cubic $SrTiO_3$, without inclusion of spin-orbit coupling. $SrTiO_3$ has an indirect band gap with the valence-band maximum at R and the conduction-band minimum at Γ. The calculated indirect band gap R-Γ is 3.47 eV and the direct band gap Γ-Γ is 3.75 eV, in good agreement with the reported experimental values of 3.25 eV and 3.75 eV,[23] and the values of 3.20 eV and 3.59 eV from recent HSE calculations using localized basis set.[24] Density functional theory using the HSE screened hybrid functional has been reported to result not only in accurate band gaps for semiconductors, but also in accurate values of deformation potentials.[25] In contrast, conventional local or semi-local functionals[12,26] are known to severely underestimate band gaps, including that of $SrTiO_3$.[22,27,28]

The lowest-energy conduction-band states in $SrTiO_3$ are derived from the Ti 3d-t_{2g} orbitals (xy, yz, zx). The bands derived from the Ti 3d-e_g orbitals ($3z^2-r^2$, x^2-y^2) lie more than 2.3 eV higher in energy. This splitting of

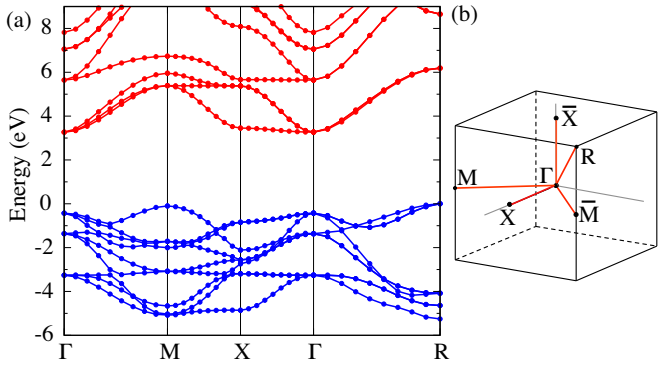

FIG. 1: (Color online) (a) Calculated band structure of cubic $SrTiO_3$ using the HSE screened hybrid functional and (b) the corresponding Brillouin zone. The zero of energy is set at the valence-band maximum at R. For the unstrained cubic phase, $\bar{M}$ is equivalent to M, and $\bar{X}$ is equivalent to X.

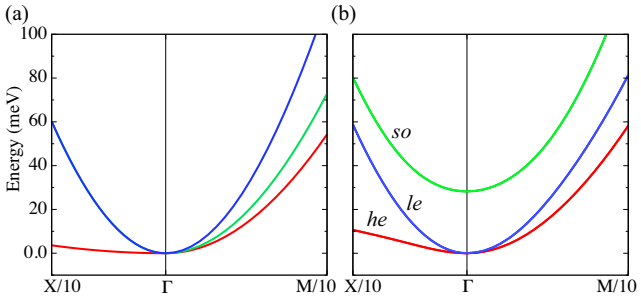

FIG. 2: (Color online) Calculated band structure of cubic $SrTiO_3$ near the conduction-band minimum at Γ, along the Γ-X and Γ-M directions. (a) Without spin-orbit coupling; (b) including spin-orbit coupling. The zero of energy is set at the conduction-band minimum.

the Ti 3*d* bands is due to the cubic crystal field produced by the six nearest-neighbor O atoms. In the absence of spin-orbit coupling, the conduction-band minimum of cubic $SrTiO_3$ is threefold degenerate at Γ. This degeneracy is broken when moving away from Γ in the X, M, or R directions, resulting in three bands with very different electron masses that are also highly anisotropic. The effects of spin-orbit coupling on the lowest conduction-band states in $SrTiO_3$ are illustrated in Fig. 2. The band structure is shown in the vicinity of the conduction-band minimum at Γ, along the Γ-X and Γ-M directions, representing two of the highest-symmetry directions. As shown in Fig. 2(b), the spin-orbit coupling breaks the threefold degeneracy at Γ, resulting in two lower-energy degenerate bands, labeled *he* and *le*, and a higher-energy split-off band, labeled *so*. The calculated spin-orbit splitting at Γ is 28 meV, in good agreement with all-electron calculations,[8] and 30% smaller than an estimated value based on the spin-orbit splitting of atomic Ti 3*d* states.[9,10]

The spin-orbit coupling has a strong effect on the electron effective mass of the lowest conduction band in $SrTiO_3$, i.e., the *he* band, as shown in Fig. 2. Table I shows that spin-orbit coupling significantly reduces the effective mass m_{he}. The masses are extracted from the inverse of the second derivative at Γ of the band energies with respect to k along the Γ-X and Γ-M directions. Particularly notable is that the *he* mass along the Γ-X direction is reduced from $6.1m_0$ to $0.99m_0$. We attribute this change to a repulsion between the *so* and the *he* bands, which is stronger at larger k values. Lifting the *so* band allows the *he* band to curve upward, resulting in a lighter mass. These results are in agreement with previous density functional calculations.[8]

The degeneracy of the *le* and *he* bands at Γ can be lifted by the presence of strain, offering the possibility of tuning effective masses. A preferential occupation of a band with a low electron mass in the transport direction will lead to higher electron mobilities. Here we discuss the effects of biaxial stress corresponding to epitaxial growth in the (001) and (110) planes. Results for biaxial stress in the (111) plane, along with a discussion of the effects of uniaxial stress along the [001], [110] and [111] directions will be reported elsewhere.

In Fig. 3(a)-(b) we show the conduction-band states along the X-Γ-$\bar{X}$ and X-Γ-M paths for $\varepsilon_{\parallel}$=−1.0% (compressive) and +1.0% (tensile) strains in the (001) plane. The strains in the perpendicular direction, obtained by energy minimization, are $\varepsilon_{\perp}$=+0.65% in the case of compressive biaxial stress, and $\varepsilon_{\perp}$=−0.65% in the case of tensile stress. According to the macroscopic theory of elasticity, for biaxial stress the ratio $\varepsilon_{\perp}/\varepsilon_{\parallel}$ is given by $-2c_{12}/c_{11}$. Our

TABLE I: Calculated electron effective masses (in units of the free-electron mass m_e) along different high-symmetry directions in cubic $SrTiO_3$ with and without inclusion of spin-orbit (SO) coupling. The mass m_{he} refers to the heavy-electron band, m_{le} to the light-electron band, and m_{so} to the spin split-off band.

	m_{he}		m_{le}		m_{so}	
	Γ-X	Γ-M	Γ-X	Γ-M	Γ-X	Γ-M
without SO	6.1	0.85	0.39	0.39	0.39	0.64
with SO	0.99	0.74	0.39	0.46	0.55	0.56

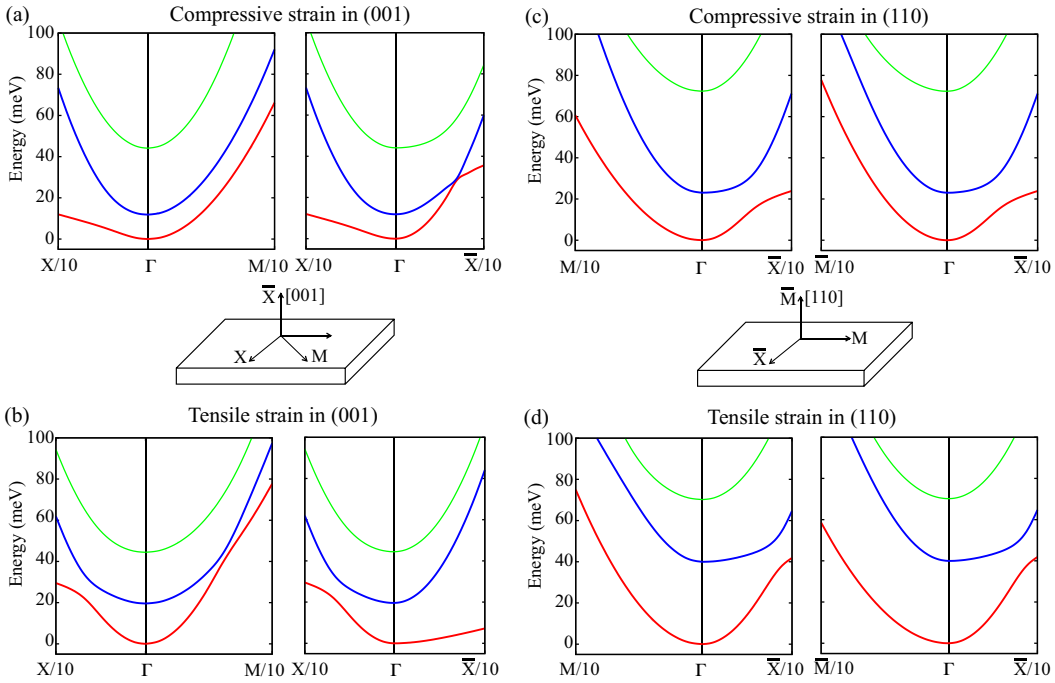

FIG. 3: (Color online) Band structure of $SrTiO_3$ near the conduction-band minimum at Γ under (a) -1% compressive and (b) +1% tensile strain in the (001) plane, plotted along the X-Γ-M and X-Γ-$\bar{X}$ directions; (c) -1% compressive and (d) +1% tensile strain in the (110) plane, plotted along the M-Γ-$\bar{X}$ and $\bar{M}$-Γ-$\bar{X}$ directions. The effects of spin-orbit coupling are included. The zero of energy is set at the conduction-band minimum.

calculated value for this ratio, 0.646, is in very good agreement with the value of 0.643 obtained from the elastic constants calculated with HSE in Ref.24, as well as with experimental values.[29]

Fig. 3(a)-(b) shows that for 1% strain in the (001) plane, either compressive or tensile, the splitting between the lowest two conduction bands is of the same order as the spin-orbit splitting. The effective mass becomes highly anisotropic under biaxial stress. For $SrTiO_3$-based heterostructures grown along the [001] direction, the relevant electronic transport directions are those parallel to the interface, and thus parallel to the plane of the strain in pseudomorphic layers, i.e., in the (001) plane, for instance along the X and M directions. For -1% compressive strain, the bands are split by 15 meV and the in-plane masses are high (see Table II). For $+1\%$ tensile strain, we observe a switch in the ordering of the bands, which are now split by 20 meV. The effective mass of the lowest conduction band is now small along the in-plane Γ-X and Γ-M directions, which are the most relevant directions for the transport. Along the perpendicular direction (Γ-$\bar{X}$), the mass is heavy. This is actually favorable, since the heavier mass along [001] allows for a higher density of states (and hence preferential occupation of the lowest band), while not affecting transport. We thus expect the electron mobility in $SrTiO_3$ under biaxial tensile stress in the (001) plane to be significantly higher than that in unstrained or biaxially compressed $SrTiO_3$.

In Fig. 3(c)-(d) we show the conduction-band states along the M-Γ-$\bar{X}$ and $\bar{M}$-Γ-$\bar{X}$ paths for $\varepsilon_{\|}=-1.0\%$ (compressive) and $+1.0\%$ (tensile) strains in the (110) plane. In this case we find that both compressive and tensile strain lead to the effective mass of the lowest band being small along the in-plane $\bar{X}$ direction, and heavier along the in-plane M and the perpendicular $\bar{M}$ directions. We note that for the tensile case the separation between the lowest and the next conduction-band state is larger (about 40 meV), indicating that it can support higher electron concentrations without occupying the next conduction-band, as compared to the compressive case.

TABLE II: Calculated electron effective masses (in units of the free-electron mass m_e) along different high-symmetry directions for the lowest-energy conduction band in biaxially stressed $SrTiO_3$. Effects of SO splitting are included. The $\bar{X}$ and $\bar{M}$ points are defined in Fig. 1(b) and the insets of Figs. 3. Values are given for compressive ($\varepsilon_\parallel$=−1%) and tensile ($\varepsilon_\parallel$=+1%) in-plane strains resulting from biaxial stress in the (001) and (110) planes.

		in-plane strain in (001) plane	
$\varepsilon_\parallel$	$m_{\Gamma-X}$	$m_{\Gamma-M}$	$m_{\Gamma-\bar{X}}$
−1.0%	0.67	0.70	0.40
+1.0%	0.42	0.42	2.2
		in-plane strain in (110) plane	
$\varepsilon_\parallel$	$m_{\Gamma-\bar{X}}$	$m_{\Gamma-\bar{M}}$	$m_{\Gamma-M}$
−1.0%	0.41	0.73	0.57
+1.0%	0.42	0.62	0.82

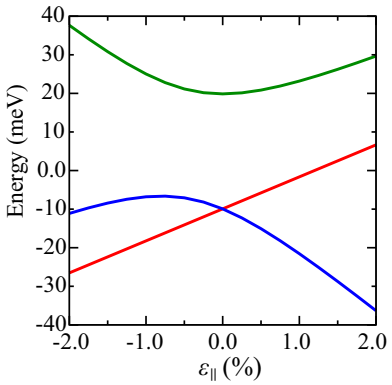

FIG. 4: (Color online) Variation of conduction bands with strain $\varepsilon_\parallel$ in the (001) plane of $SrTiO_3$. For tensile strain, the lowest band maintains mainly light-electron character and exhibits effective mass for transport along the in-plane directions.

We also determined the deformation potentials b and d related to deformations of tetragonal and trigonal symmetry, respectively. Using an analogy to the hole (valence) bands in zinc-blende semiconductors,[30] these parameters were calculated by inspecting the band structure when strain is applied. Neglecting spin-orbit coupling, the lowest energy conduction bands split into twofold and onefold states at Γ, with energy splittings of $\frac{3}{2}|\delta E_{001}|$ and $\frac{3}{2}|\delta E_{111}|$ for tetragonal and trigonal deformations, where the quantities δE_{001} and δE_{111} are expressed in terms of deformation potentials and strain components as in Eqs. (13) and (14) of Ref.30. The resulting deformation potentials are b=−0.51 eV and d=−2.15 eV. We have verified that, using these deformation potentials, we can reproduce the energy splittings of the various bands in the presence of spin-orbit splitting as calculated explicitly from first principles. As an example, we plot in Fig. 4 the variation of the conduction bands as a function of biaxial strain $\varepsilon_\parallel$ in the (001) plane in $SrTiO_3$ using the calculated b parameter and including the effects of spin-orbit splitting, following Eqs. (12) in Ref.30. Although the character of the bands becomes mixed when strain is applied, for tensile strain the lowest band remains mainly *le*-like and exhibits low effective mass along the in-plane directions [Fig. 3(b)].

The effects of strain on the conduction-band states in $SrTiO_3$ offer great opportunities for the design of electronic devices. Tensile strain in $SrTiO_3$ can be induced by growth on substrates with larger lattice constants. For instance, the growth of 25-nm thick $SrTiO_3$ on the (110) plane of $DyScO_3$ has been recently reported,[31] resulting in in-plane tensile strains of 1.1% and 1.2% due to the orthorhombic structure of the substrate. However, the focus of that work was not on transport properties. Other possible substrates with lattice constants larger than that of $SrTiO_3$ are $TbScO_3$ with pseudocubic lattice constants a_p=3.960 Å and c_p=3.959 Å, $GdScO_3$ (a_p=3.970 Å and c_p=3.966 Å),[32] $KTiO_3$ (a=3.989 Å), (Ba,Sr)TiO_3 with 3.90≤ a ≤ 4.00 Å, and Pb(Zr,Ti)O_3 with $a \geq$ 3.97 Å.[19,33]

In summary, based on first-principles calculations we find that the effective mass of electrons in the transport direction can be lowered by subjecting $SrTiO_3$ films to tensile biaxial stress in the (001) or (110) planes, which can be accomplished by pseudomorphic growth on suitable substrates. The lower electron effective mass should result in significantly higher electron mobilities.

We are grateful to B. Jalan, S. Stemmer, and Q. Yan for useful discussions. This work was supported by the Army Research Office (W911-NF-09-1-0398 and W911-NF-11-1-0232) and by the NSF MRSEC Program (DMR05-20415). It made use of the CNSI Computing Facility under NSF grant No. CHE-0321368, and the Ranger supercomputer

from the TeraGrid computing resources supported by the NSF under grant No. DMR070072N.

[1] A. Ohtomo, D. A. Muller, J. L. Grazul, and H. Y. Hwang, Nature **419**, 378 (2002).
[2] A. Ohtomo, H. Hwang, Nature **427**, 423 (2004).
[3] J. Mannhart, D. H. A. Blank, H. Y. Hwang, A. J. Millis, and J. M. Triscone, MRS Bull. **33**, 1027 (2008).
[4] J. Son, P. Moetakef, B. Jalan, O. Bierwagen, N. J. Wright, R. Engel-Herbert, and S. Stemmer, Nat. Mater. **9**, 482 (2010).
[5] T. Okuda, K. Nakanishi, S. Miyasaka, and Y. Tokura, Phys. Rev. B **63**, 113104 (2001).
[6] M. Ahrens, R. Merkle, B. Rahmati, J. Maier, Physica B **393**, 239 (2007).
[7] W. Wunderlich, H. Ohta, and K. Koumoto, Physica B **404**, 2202 (2009).
[8] M. Marques, L. K. Teles, V. Anjos, L. M. R. Scolfaro, J. R. Leite, V. N. Freire and G. A. Farias, and E. F. da Silva, Jr., Appl. Phys. Lett. **82**, 3074 (2003).
[9] L. F. Mattheiss, Phys. Rev. B **6**, 4718 (1972).
[10] L. F. Mattheiss, Phys. Rev. B **6**, 4740 (1972).
[11] B. Jalan, S. J. Allen, G. E. Beltz, P. Moetakef, and S. Stemmer, Appl. Phys. Lett. **98**, 132102 (2011).
[12] P. Hohenberg and W. Kohn, Phys. Rev. **136**, B864 (1964). W. Kohn and L. J. Sham, Phys. Rev. **140**, A1133 (1965).
[13] J. Heyd, G. E. Scuseria, and M. Ernzerhof, J. Chem. Phys. **118**, 8207 (2003); erratum: J. Chem. Phys. **124**, 219906 (2006).
[14] G. Kresse and J. Furthmüller, Phys. Rev. B 54, 11169 (1996).
[15] G. Kresse and J. Furthmüller, Comput. Mat. Sci. 6, 15 (1996).
[16] P. E. Blöchl, Phys. Rev. B **50**, 17953 (1994).
[17] G. Kresse and D. Joubert, Phys. Rev. B 59 (1999) 1758.
[18] L. Cao, E. Sozontov, and J. Zegenhagen, phys. stat. sol. (a) **181**, 387 (2000).
[19] O. Muller, R. Roy, *The Major Ternary Structural Families*, (Springer, NewYork-Heidelberg-Berlin, 1974).
[20] F. He, B. O. Wells, Z.-G. Ban, S. P. Alpay, S. Greiner, S. M. Shapiro, W. Si, A. Clark, and X. X. Xi, Phys. Rev. B **70** 235405 (2004).
[21] F. He, B. O. Wells, and S. M. Shapiro, Phys. Rev. Lett. **94**, 176101 (2005).
[22] R. Wahl, D. Vogtenhuber, and G. Kresse, Phys. Rev. B **78**, 104116 (2008).
[23] K. van Benthem, C. Elsässer, and R. H. French, J. Appl. Phys. **90**, 6156 (2001).
[24] F. El-Mellouhi, E. N. Brothers, M. J. Lucero, and G. E. Scuseria, Phys. Rev. B **84**, 115122 (2011).
[25] Q. Yan, P. Rinke, M. Scheffler, and C. G. Van de Walle, Appl. Phys. Lett. **95**, 121111 (2009).
[26] J. P. Perdew, K. Burke, and M. Ernzerhof, Phys. Rev. Lett. **77**, 3865 (1996).
[27] S. Piskunov, E. Heifets, R.I. Eglitis, G. Borstel, Comp. Mater. Sci. **29**, 165 (2004).
[28] W. Luo, W. Duan, S. G. Louie, and M. L. Cohen, Phys. Rev. B **70**, 214109 (2004).
[29] R. O. Bell and G. Rupprecht, Phys. Rev. **129**, 90 (1963).
[30] C. G. Van de Walle, Phys. Rev. B **39**, 1871 (1989).
[31] H. Ma, J. Levy, M. D. Biegalski, S. Trolier-McKinstry, and D. G. Schlom, J. Appl. Phys. **105**, 014102 (2009).
[32] R. Uecker, B. Velickov, D. Klimm, R. Bertram, M. Bernhagen, M. Rabea, M. Albrecht, R. Fornari, D.G. Schlom, J. Cryst. Growth. **310**, 2649 (2008).
[33] D. G. Schlom, L.-Q. Chen, X. Pan, A. Schmehl, and M. A. Zurbuchen, J. Am. Ceram. Soc. **91**, 2429 (2008).